

The Energetic and Structural Effects of Steric Crowding in Phosphate and Dithiophosphinate Complexes of Lanthanide Cations M^{3+} : A Computational Study

Christian Boehme and Georges Wipff^{*[a]}

Abstract: Metal–ligand binding strength and selectivity result from antagonistic metal–ligand M–L attractions and ligand–ligand L–L repulsions. On the basis of quantum-mechanical (QM) calculations on lanthanide complexes, we show that this interplay determines the binding affinities in the gas phase. In the series of $[ML_3]$ complexes (M = La, Eu, and Yb) with negatively charged phosphoryl ligands $L^- = (MeO)_2PO_2^-$ and $Me_2PS_2^-$, the binding energies follow the order $Yb^{3+} > Eu^{3+} > La^{3+}$ for a given ligand, and

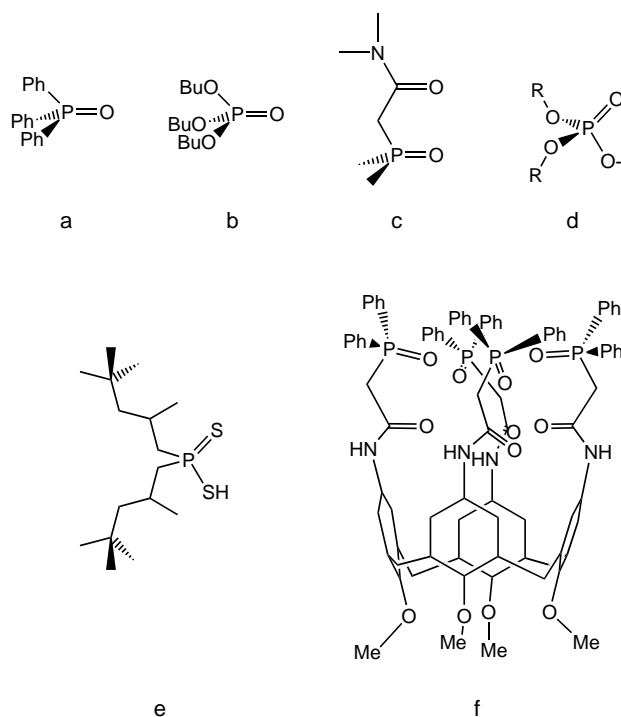
$(MeO)_2PO_2^- > Me_2PS_2^-$ for a given cation. However, adding a neutral LH ligand to $[ML_3]$ changes the order to $Eu^{3+} > Yb^{3+} > La^{3+}$ for the oxygen ligand and $La^{3+} > Eu^{3+} > Yb^{3+}$ for the sulfur ligand, indicating that steric strain in the first coordination sphere is largest for the smallest cation and for sulfur

Keywords: ab initio calculations · ion separation · lanthanides · molecular dynamics · phosphoryl ligands

binding sites. We investigated the question of additional hydration of the $[ML_3LH]$ complexes in aqueous solution by molecular dynamics (MD) simulations, using two sets of atomic charges. It was found that pairwise additive potentials overestimate the coordination and hydration numbers of the cations, while adding polarization energy terms for the ligands yields better agreement between QM and MD results and supports the concept of steric strain in the first coordination sphere.

Introduction

Organophosphorus ligands L are of great importance in the field of liquid–liquid extraction of lanthanide and actinide ions from aqueous solutions.^[1–3] The ligands used (see Scheme 1) range from simple monodentate compounds like TPPO and TBP to bidentate types like CMPO, phosphates, and the dithiophosphinic acid Cyanex-301,^[4–7] to complex systems like cavitands or the recently developed calixarenes,^[8–10] which utilize phosphoryl binding groups anchored to a lipophilic platform. While most ligands used employ oxygen as binding site, recently developed compounds like the aforementioned Cyanex-301 show that sulfur can be a good alternative. The fundamental idea is that ligands based on sulfur, which is a “soft” base compared to oxygen,



Scheme 1. Typical phosphoryl-containing ligands: a) TPPO, b) TBP, c) CMPO, d) alkylphosphates, e) CYANEX-301, f) CMPO–calixarene.

[a] Prof. G. Wipff, Dr. C. Boehme
Laboratoire MSM, Institut de Chimie
UMR CNRS 7551, Université Louis Pasteur
4, rue B. Pascal, 67 000 Strasbourg (France)
Fax: (+33) 388-416104
E-mail: wipff@chimie.u-strasbg.fr

Supporting information for this article is available on the WWW under <http://www.wiley-vch.de/home/chemistry/> or from the author.

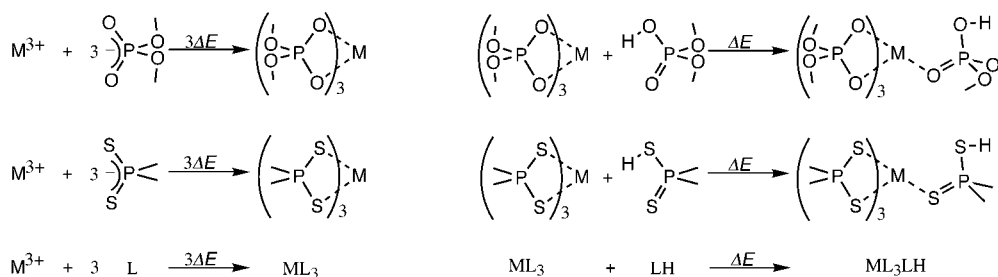
may not yield binding energies as high as oxygen-based ligands, but may be more selective regarding cations of different size and “hardness”.^[11–13]

The great number of possible candidates makes choosing the right ligands for synthesis and testing them in the liquid–liquid extraction of lanthanides and actinides very difficult. Experimental results can serve as a guideline, but a more general understanding of the different factors involved is desirable. Quantum-mechanical (QM) and classical force-field (molecular mechanics, MM, and molecular dynamics, MD) calculations are an important source of information on these factors. Our group has undertaken QM studies of lanthanide complexes of organophosphorus ligands with both oxygen and sulfur as binding sites.^[14,20] The results show that oxygen binding sites generally yield higher binding energies than sulfur binding sites. One of the most interesting realizations from these studies, however, is that the effects of steric repulsion in the first coordination shell of the metal cation on the ligands’ cation selectivity can be stronger than all other effects, including the electronic influence of the organic substituents of the phosphorus atom. An important issue is the relation between cation coordination number (CN) and ligand binding strength and selectivity. For instance, the $[\text{Me}_2\text{PS}_2]^-$ ligand interacts more strongly with Yb^{3+} than with Eu^{3+} in 1:1 complexes, as expected from the relative cation sizes and hardnesses. This trend is followed up to a 1:3 $[\text{ML}_3]$ stoichiometry. However, adding a fourth ligand is more favorable for Eu^{3+} than for Yb^{3+} . We attributed this reversal to steric repulsions within the first coordination sphere.^[19,20] We notice that the resulting CN of 8 is the commonly observed value for Yb^{3+} (e.g. with water or acetonitrile ligands), and lower than the usual CN of 9 for Eu^{3+} .^[21] However, variations of the CN are observed for a given metal as a function of the charge and size of its ligands or coordinated counterions. Generally bidentate ligands yield higher CNs than monodentate ones. Solid-state structures with up to four bidentate R_2PS_2^- ligands are common for lanthanide cations (see discussion in ref. [20]), while up to five NO_3^- anions can be found around Eu^{3+} .^[22] The energetic features of such an accumulation of negative charges around the cation remain to be investigated.

In this study we want to compare the quantum-mechanical (QM) binding energies and cation selectivities of the hard phosphate ligand $[(\text{MeO})_2\text{PO}_2]^-$ (denoted P^-) with those of the softer dithiophosphinate ligand $[\text{Me}_2\text{PS}_2]^-$ (denoted TP^-), both ligands are referred to as L^- , see Scheme 2). The per-ligand binding energies in the $[\text{ML}_3]$ ($\text{M}^{3+} = \text{La}^{3+}, \text{Eu}^{3+}, \text{Yb}^{3+}$,

Scheme 2) complexes are dominated by the high binding energy of the first ligand and therefore measure the strength of the electronic and coulombic interactions between ligand and cation and how these interactions influence the cation selectivity of L^- . The three chosen lanthanide cations, lanthanum(III), europium(III), and ytterbium(III) represent cations of different size and hardness, La^{3+} being the largest and softest, Yb^{3+} the smallest and hardest cation. One protonated ligand LH ($(\text{MeO})_2\text{POOH}$, denoted PH , or Me_2PSSH , denoted TPH) is added to the $[\text{ML}_3]$ complexes, forming complexes of the type $[\text{ML}_3\text{LH}]$ (Scheme 2). The resulting interaction energy is strongly influenced by steric effects. Furthermore the protonated ligand has one stronger binding site (the unprotonated oxygen or sulfur atom) and one weaker binding site (the protonated oxygen or sulfur atom). It is of interest whether the weaker site will also form a bond to the metal cation, that is, whether the steric repulsion in the first coordination sphere is weaker than the possible bond. The choice of LH to test the steric effects relates to the liquid–liquid extraction process of lanthanide cations by hydrophobic LH ligands, where three of them exchange their proton with an extracted metal, forming the $[\text{ML}_3]$ complex.^[6,7] From a mechanistic point of view, we suggested that LH accumulates at the “oil”–water interface where complexation takes place.^[23] The complex thus forms in a liquid medium where LH is concentrated and may additionally bind to the neutral $[\text{ML}_3]$ complex, stripping coordinated water molecules and thus facilitating its extraction into the “oil” phase. The binding of LH to ML_3 also mimics the synergistic effects of neutral phosphorylated ligands like TBP .^[7]

In order to test whether the $[\text{ML}_3\text{LH}]$ complexes are hydrophobic enough to be extracted, or whether they still display a large affinity for water in the first coordination sphere of the metal, it would be desirable similarly to add water molecules and fully optimize the $[\text{ML}_3\text{LH}(\text{H}_2\text{O})_n]$ “supermolecules” until saturation is reached. This supermolecule approach requires computer means beyond our presently available resources and is not yet sufficient to account for solvent dynamics. We therefore address the question of hydration of $[\text{ML}_3\text{LH}]$ using MD simulations in a box of explicitly represented water molecules. This requires a simplified ball-and-stick representation of the system, with fixed atomic charges and “atom sizes”. Thus, electronic reorganization (charge transfer and polarization effects) upon coordination is not represented. On the other hand, the simplified approach allows us to replace the methyl and methoxy substituents by the more realistic substituents phenyl



Scheme 2. Definition of ligand binding energies ΔE .

and phenoxy. From a methodological point of view, it is also important to test whether QM and MD approaches yield the same trends concerning water coordination to $[\text{ML}_3\text{LH}]$. Beyond the field of ion extraction, this is crucial for simulations related to photophysical aspects and relaxation time of coordinated water.^[24–27] Thus, in the second part of the paper, we report MD results of $[\text{ML}_3\text{LH}]$ complexes in water with the aim of determining the number of additional water molecules as a function of the cation size, nature of the ligands, and resulting steric crowding in the first coordination sphere.

Computational Methods

The quantum-mechanical studies were performed with the package Gaussian 98.^[28] The compounds studied were fully optimized at the Hartree–Fock level of theory. On oxygen, sulfur, phosphorus, and carbon, the Dunning–Huzinaga double-zeta-plus polarization basis sets were used.^[29] A basis set of the same type without polarization function was used on hydrogen. A quasirelativistic ECP of the Stuttgart group was used on the lanthanides, together with the affiliated (5/4/3) valence basis,^[30, 31] to which one f-function with an exponent optimized by Frenking et al. was added.^[32] The suitability of this approach, which does not include the effects of electron correlation, for the studied compound types has been discussed in our previous works.^[16, 18–20]

The simulations of the $[\text{ML}_3\text{LH}]$ complexes in the gas phase and in water were performed with AMBER 4.1 software.^[33] The potential energy function U includes bond, angle, and dihedral terms and pairwise additive 1-6-12 (electrostatic and van der Waals) interactions of the Lennard-Jones type between non-bonded atoms [Eq. (1)].

$$U = \sum_{\text{bonds}} K_i (r - r_{\text{eq}})^2 + \sum_{\text{angles}} K_\theta (\theta - \theta_{\text{eq}})^2 + \sum_{\text{dihedrals}} \sum_n V_n (1 + \cos n\phi) + \sum_{i < j} [q_i q_j / R_{ij} - 2\epsilon_{ij} (R_{ij}^*/R_{ij})^6 + \epsilon_{ij} (R_{ij}^*/R_{ij})^{12}] \quad (1)$$

Atom types are given in Figure S1 (Supporting Information). The corresponding parameters were taken from the AMBER force field^[34] where the size of atoms and cations depends on the parameters R^* , ϵ . The cation parameters ($R_{\text{La}}^* = 2.105$; $R_{\text{Eu}}^* = 1.852$; $R_{\text{Yb}}^* = 1.656$ Å; $\epsilon_{\text{La}} = 0.06$; $\epsilon_{\text{Eu}} = 0.05$; $\epsilon_{\text{Yb}} = 0.04$ kcal mol⁻¹), fitted from free energies of hydration, are from ref. [35]. Two sets of atomic charges were used for the electrostatic interactions. The first one (MK) uses the Merz–Kollman atomic charges derived from our QM calculations on the isolated L⁻ and LH ligands in conjunction with a +3 charge on the cations (Figure S1). The second set uses Mulliken charges on the $[\text{ML}_3\text{LH}]$ complexes, thus somewhat taking into account the electronic redistribution in the complex. They are given in Table S1. The water molecules were represented explicitly by means of the TIP3P model.^[36] The non-bonding interactions were calculated with a residue-based cutoff of 12 Å. Some simulations (MK+pol) were repeated including polarization effects, with the procedure described in ref. [37] and the Applequist atomic polarizabilities ($\alpha_{\text{C}} = 0.88$, $\alpha_{\text{H}} = 0.13$, $\alpha_{\text{O}} = 0.46$, $\alpha_{\text{S}} = 1.70$, $\alpha_{\text{P}} = 1.90$ Å³).^[38]

Each complex was energy-minimized in the gas phase and immersed at the center of a cubic box of about 30 Å length, containing about 1000 water molecules, simulated with 3D periodic boundary conditions. After 10000 steps of energy minimization, 50 ps of MD were performed, keeping the complex frozen (BELLY option of AMBER). Then a free MD was run for 250 ps (calculations without polarization) or 150 ps (calculations MK+pol with polarization) at 300 K

and at constant volume. In order to keep the complex as hydrophobic and tight as possible, we constrained the seven M–S and M–O distances at the average equilibrium values after minimization in water, with a restraining potential of 10 kcal mol⁻¹. No constraint was applied to the M–SH and M–OH distances.

The results were analyzed with MDS and DRAW.^[39, 40] The hydration numbers of the complexed cations were obtained by integration of the ion–O_{water} radial distribution functions (RDFs), skipping the first 30 ps of the trajectories.

Results and Discussion

1. QM results for the $[\text{ML}_3]$ and $[\text{ML}_3\text{LH}]$ complexes in the gas phase

1.1. The QM-derived geometries of the complexes: The structures of the calculated complexes can be seen in Table 1 and Figure 1 ($[\text{ML}_3]$ -type complexes) and 2 ($[\text{ML}_3\text{LH}]$ -type complexes). In all $[\text{ML}_3]$ complexes, the MS_6 and MO_6 moieties are of approximately D_3 symmetry where the phosphorus atoms form a planar triangle around the metal cation with the oxygen and sulfur atoms in turn above and below this plane. Interestingly the dithiophosphate (TP^-) complexes have identical M–S distances, while the phosphate (P^-) complexes are less regular, with M–O bond-length differences of up to 0.032 Å, related to the asymmetrical arrangement of the O–methyl groups and induced stereo-electronic effects.^[41] We did not systematically explore the different orientations of these groups, but the corresponding energy changes are expected to be small compared with the metal–ligand binding energies ΔE .

The addition of a protonated LH ligand leads to different structure types. In all cases most of the bonds of the ligands L⁻ are elongated because the new ligand LH competes with them as a donor, and enhances repulsions in the first coordination shell. In the case of the LaP_3PH complex only, the PH ligand is bidentate and forms two comparatively long coordinate bonds to the metal. As the protonated oxygen is only a weak donor, the binding energy of PH to the LaP_3 complex should be low (vide infra). Nevertheless, the repulsion between the oxygen atoms in the first coordination sphere of the lanthanum cation is still not high enough to compete with the metal–ligand attractions. This contrasts with all other complexes studied, in

Table 1. QM-optimized $[\text{ML}_3]$ and $[\text{ML}_3\text{LH}]$ complexes: M–X distances in Å (M = La, Eu, Yb; X = O, S binding sites).

Complex ^[a]	M–X1	M–X1'	M–X2	M–X2'	M–X3	M–X3'	M–X4	M–X4'
$[\text{LaP}_3]$	2.483	2.491	2.513	2.508	2.510	2.518		
$[\text{EuP}_3]$	2.376	2.383	2.407	2.400	2.406	2.408		
$[\text{YbP}_3]$	2.279	2.284	2.311	2.302	2.309	2.309		
$[\text{LaP}_3\text{PH}]$	2.603	2.521	2.563	2.545	2.512	2.587	2.699	2.891
$[\text{EuP}_3\text{PH}]$	2.432	2.438	2.458	2.429	2.431	2.561	2.371	4.092
$[\text{YbP}_3\text{PH}]$	2.393	2.310	2.356	2.435	2.331	2.350	2.282	4.022
$[\text{LaTP}_3]$	3.024	3.024	3.024	3.024	3.024	3.024		
$[\text{EuTP}_3]$	2.914	2.914	2.914	2.914	2.914	2.914		
$[\text{YbTP}_3]$	2.818	2.818	2.818	2.818	2.818	2.818		
$[\text{LaTP}_3\text{TPH}]$	3.099	3.029	3.078	3.046	3.054	3.112	3.226	5.237
$[\text{EuTP}_3\text{TPH}]$	3.011	2.909	2.983	2.948	2.959	3.022	3.121	4.965
$[\text{YbTP}_3\text{TPH}]$	2.946	2.808	2.906	2.868	2.880	2.944	3.020	4.864

[a] $\text{P}^- = (\text{CH}_3\text{O})_2\text{POO}^-$, $\text{TP}^- = (\text{CH}_3)_2\text{PSS}^-$.

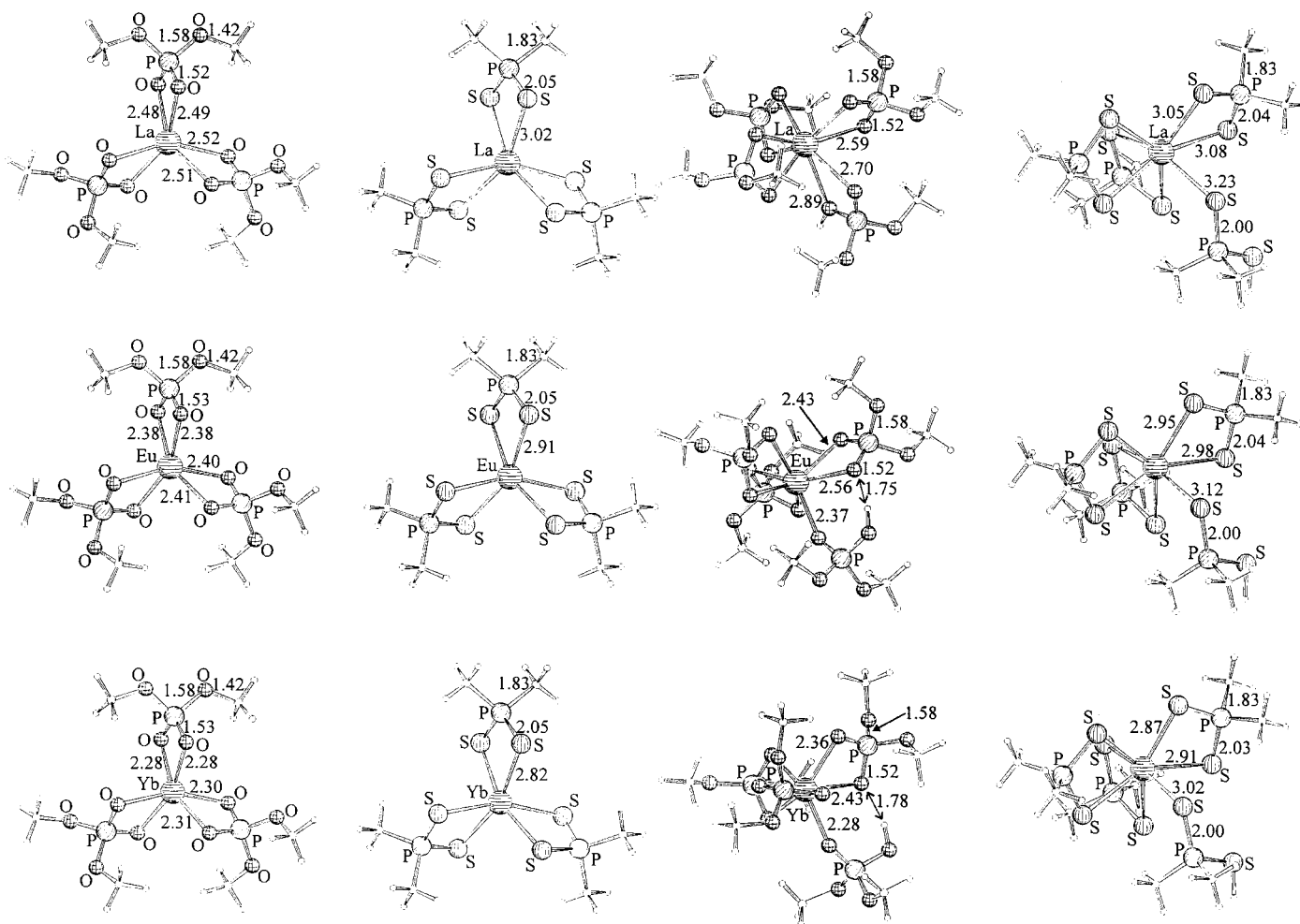


Figure 1. QM-optimized structures of the $[ML_3]$ complexes, with $M = \text{La}$ (top), Eu (middle), and Yb (bottom) and $L^- = \text{P}^-$ (left) and TP^- (right).

Figure 2. QM-optimized structures of the $[ML_3LH]$ complexes, with $M = \text{La}$ (top), Eu (middle), and Yb (bottom) and $L^- = \text{P}^-$ (left) and TP^- (right).

which the LH ligand is monodentate, bound by the unprotonated oxygen or sulfur atom, because of enhanced ligand–ligand repulsions. These repulsions are higher with the smaller cations or/and the larger binding atoms. One should note that the one $M\text{--}O_{\text{LH}}$ bond formed is shorter than the other $M\text{--}O_{\text{L}}$ bonds in the case of the phosphate $[\text{EuP}_3\text{PH}]$ and $[\text{YbP}_3\text{PH}]$ complexes where PH is monodentate, but longer in $[\text{LaP}_3\text{PH}]$ where LH is bidentate. In the three dithiophosphinate $[\text{MTP}_3\text{TPH}]$ complexes, where TPH is also monodentate, the $M\text{--}S_{\text{LH}}$ bond is longer than the $M\text{--}S_{\text{L}}$ bonds. There is thus no simple relationship between the charge of the coordinated ligand and the corresponding distances to the metal.

In the phosphate complexes $[\text{EuP}_3\text{PH}]$ and $[\text{YbP}_3\text{PH}]$, the proton attached to the oxygen atom in the ligand PH forms a weak hydrogen bond to a coordinated oxygen of a neighboring ligand P^- . That a noticeable interaction does indeed occur can be seen firstly from the $\text{O}\cdots\text{H}$ distances (1.751 Å and 1.784 Å, respectively). Secondly, the $M\text{--}O$ bonds formed by the proton-acceptor oxygen atoms are elongated by about 0.1 Å in EuP_3PH and by about 0.04 Å in YbP_3PH compared with the non-hydrogen-bonded $M\text{--}O$ bond. No such interaction can be found in the corresponding dithiophosphinate complexes, probably owing to the poorer ability of sulfur atoms to form hydrogen bonds and less favorable arrangement of the ligands.

1.2. The QM-derived binding energies of the complexes: The relevant energy data for the complexes studied can be found in Table 2. Definitions for ΔE can be found in Scheme 2. The high ΔE values per ligand ($>300 \text{ kcal mol}^{-1}$) of the $[ML_3]$ complexes are dominated by the coulombic attraction between the positively charged metal cation and the negatively charged ligand. The further influences are size and hardness of the metal cations and the ligands' binding sites. Both the dithiophosphinate ligand TP^- and the phosphate ligand P^- “prefer” the smaller and harder cations; in other words, the binding energies rise in the order $\text{La}^{3+} < \text{Eu}^{3+} < \text{Yb}^{3+}$. This Yb/La preference is somewhat higher in the case of the hard phosphate ligand (-32.9 vs $-29.5 \text{ kcal mol}^{-1}$), but the difference from the presumably soft sulfur ligand is small.

The picture gets much more complicated for the addition of the neutral LH ligand. In the case of the phosphate ligand PH the binding energy rises from La^{3+} to Eu^{3+} but then falls for Yb^{3+} (see $\Delta\Delta E_{\text{L}}$, Table 2), making the order of cation selectivity $\text{La}^{3+} < \text{Yb}^{3+} < \text{Eu}^{3+}$. This change may be ascribed to steric crowding, that is, to the repulsion between the binding sites in the first coordination sphere of the metal cations. If we assume that the La/Yb cation selectivity is comparable for the PH and P^- ligands (as is the La/Eu selectivity), the difference $\Delta\Delta E$ in per-ligand binding energies

Table 2. Reaction energies ΔE [kcal mol⁻¹] in the gas phase from QM calculations (see definitions in Scheme 2). $\Delta\Delta E_L$ are the differences between ΔE 's as a function of M for a given ligand. $\Delta\Delta E_M$ are the differences between sulfur- and oxygen-containing ligands for a given metal.

Complexes ^[a]	ΔE	$\Delta\Delta E_L$	$\Delta\Delta E_M$
[LaP ₃]	-320.0	0.0	0.0
[EuP ₃]	-336.4	-16.4	0.0
[YbP ₃]	-352.9	-32.9	0.0
[LaP ₃ PH]	-21.8	0.0	0.0
[EuP ₃ PH]	-35.0	-13.2	0.0
[YbP ₃ PH]	-30.6	-8.8	0.0
[LaTP ₃]	-306.3	0.0	+13.7
[EuTP ₃]	-321.4	-15.1	+15.0
[YbTP ₃]	-335.8	-29.5	+17.1
[LaTP ₃ TPH]	-4.9	0.0	+16.9
[EuTP ₃ TPH]	-1.0	+3.9	+34.0
[YbTP ₃ TPH]	+4.0	+8.9	+34.6

[a] See Table 1.

ΔE between LaP₃PH and YbP₃PH should be about the same as between LaP₃ and YbP₃, about 30 kcal mol⁻¹. It is, however, only about 10 kcal mol⁻¹; this means that steric repulsions are roughly 20 kcal mol⁻¹ larger in YbP₃PH than in LaP₃PH.

In the dithiophosphinate complexes the same effect leads to a reversal of the metal cation selectivity; the binding energies of the TPH ligand rise from the smallest to the largest cation, Yb³⁺ < Eu³⁺ < La³⁺. By the same argument as in the case of the phosphate complexes, the strength of the steric effect can be estimated to be about 20 kcal mol⁻¹ in [EuTP₃TPH] and about 40 kcal mol⁻¹ in [YbTP₃TPH], much higher than in the corresponding phosphate complexes. In [YbTP₃TPH] it is high enough to make the TPH-Yb bond endothermic. The estimated strength of steric effects of 20 kcal mol⁻¹ for [EuTP₃TPH] is also obtained if one assumes that the energy gain $\Delta\Delta E$ from [LaTP₃TPH] to [EuTP₃TPH] is about the same as from [LaP₃PH] to [EuP₃PH] (as is true for the corresponding [ML₃] complexes), about 15 kcal mol⁻¹. Instead there is a binding energy loss of about 5 kcal mol⁻¹, which again hints at an approximate steric repulsion of about 20 kcal mol⁻¹.

2. Molecular dynamics investigations of the 1:4 complexes in the gas phase and in aqueous solution: In order to obtain more information on the role of the steric strain in the first shell of the lanthanide ions, we tried to determine the number of additional water molecules that can coordinate to the neutral

1:4 ML₃LH complexes in aqueous solution. Here, the ligands are modeled with phenyl substituents—as used in the more hydrophobic ligands of Modolo et al.^[6]—instead of methyl substituents. Simulations were performed with three different representations of the electrostatic interactions. The first two (*i*) and (*ii*) are standard and use coulombic interactions only (1-6-12 potentials), while the third (*iii*) includes an additional polarization energy contribution. Model (*i*) uses the Merz–Kollman (MK) charges on the ligands, in conjunction with a +3 charge on the cation. This simple model, which assumes the transferability of atomic charges from one cation to the other, and from uncomplexed ligands to complexed ones, is widely used to simulate ion complexation in solution. Simulations (*ii*) use the Mulliken atomic charges, derived from the QM optimizations on the [ML₃LH] complexes. They thus vary from one system to the other, and to some extent reflect the electronic reorganization that takes place upon complexation: electron transfer from the ligands to the cation, and polarization of the ligand by other species (mostly the cation). The set (*iii*) of simulations (MK+pol), performed on selected systems, uses the MK charges on the ligands and a +3 cation, plus a polarization energy term for the atoms of the ligands. As shown in a recent study in acetonitrile solution, such a polarization correction leads to lower coordination numbers compared with those obtained with the 1-6-12 potentials only, and is also in better agreement with experiment.^[42]

We started with a molecular mechanics (MM) optimization of the [ML₃LH] complexes. The MK and Mulliken charges led to nearly identical structures where all L⁻ and LH ligands are bound to the metal. Table 3 shows that the M–L distances are shorter than in the QM structures, indicating that some van der Waals R^* are somewhat too small, and/or that metal–ligand attractions are exaggerated with AMBER. The differences are larger than 0.2 Å in some cases, but considering the simplicity of the potentials used and that the ligands in the MD simulations are phenyl-substituted, while they are methyl-substituted in the QM calculations, the quality of the AMBER results is satisfactory. We notice that the cation size, fitted in an aqueous environment,^[35] may be less appropriate for ligands other than water.^[43]

During the MD simulations in the gas phase, the neutral LH ligands remained coordinated to the metal. One exception concerns the MK+pol results for the [EuTP₃TPH] and [YbTP₃TPH] systems, in which TPH spontaneously dissociated. Such dissociation is consistent with the QM results according to which the binding energy of LH is nearly zero or

Table 3. M–X distances in Å (M = La, Eu, Yb; X = O, S binding sites) from the unconstrained AMBER MM optimizations with MK charges in the gas phase. Number of coordinated water molecules (CN_w) from the MD simulations in water, with MK (CN_{w,MK}) and Mulliken (CN_{w,Mul}) charges.

Complex ^[a]	M–X1	M–X1'	M–X2	M–X2'	M–X3	M–X3'	M–X4	M–X4'	CN _{w,MK}	CN _{w,Mul}
[LaP ₃ PH]	2.53	2.54	2.53	2.55	2.51	2.66	2.52	4.13	3.1	2.5
[EuP ₃ PH]	2.33	2.32	2.32	2.33	2.32	2.36	2.31	4.39	3.0	1.8
[YbP ₃ PH]	2.15	2.16	2.16	2.17	2.17	2.20	2.15	4.27	2.0	1.0
[LaTP ₃ TPH]	2.82	2.78	2.83	2.83	2.81	2.80	2.97	3.32	2.9	2.0
[EuTP ₃ TPH]	2.65	2.59	2.66	2.67	2.64	2.64	2.79	3.55	2.4	1.5
[YbTP ₃ TPH]	2.52	2.49	2.45	2.50	2.46	2.52	2.83	5.35	2.0	1.0

[a] See Table 1.

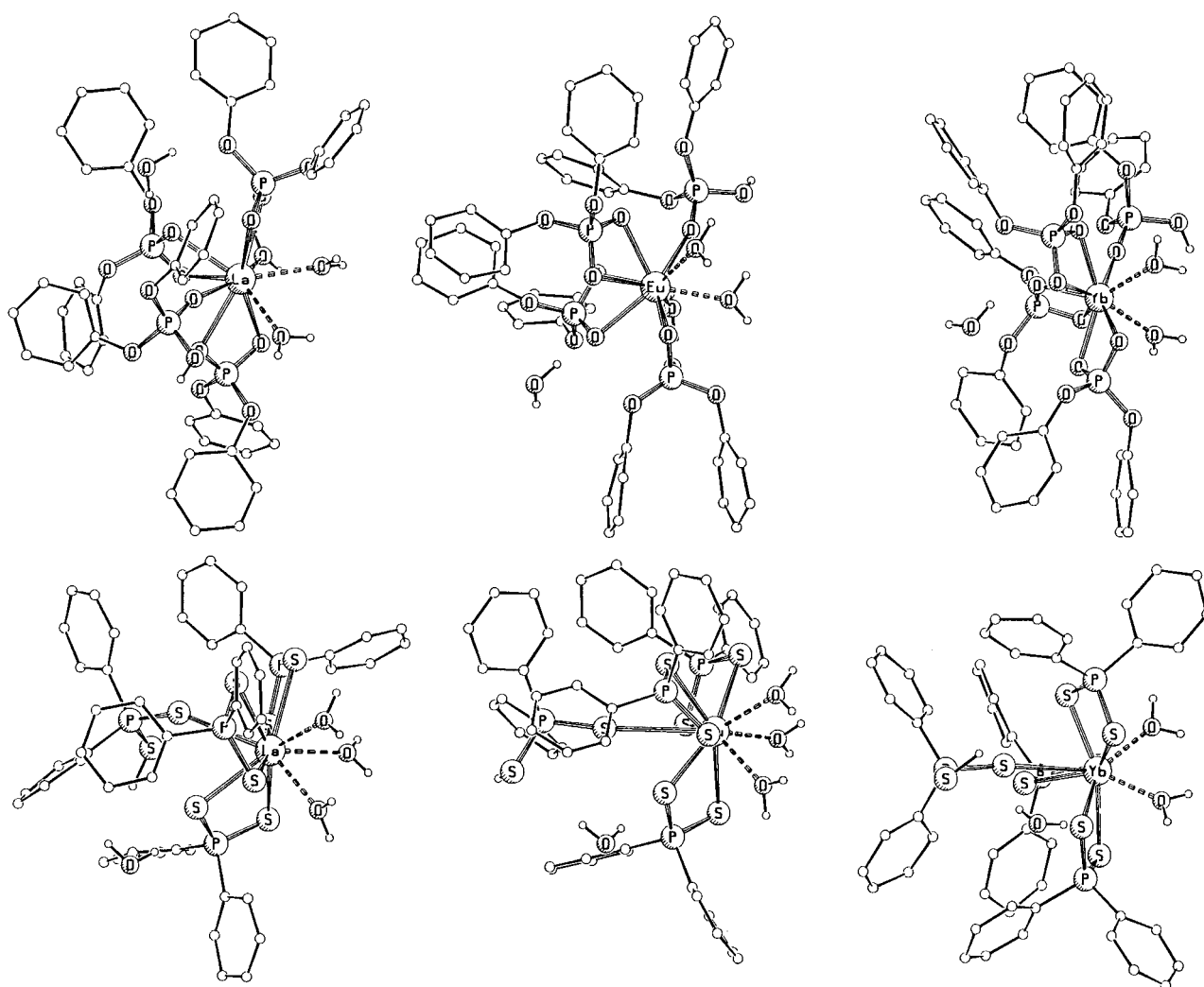


Figure 3. $[ML_3LH]$ complexes, MD simulated in water (using MK charges and constrained M–S or M–O binding distances). Snapshots with selected water molecules, with M = La (left), Eu (middle), and Yb (right) and $L^- = P^-$ (top) and TP^- (bottom). Note that the ligands bear phenyl rather than methyl substituents.

positive in these complexes, but negative in all others. It also supports the thesis of the greatest steric crowding with the smallest cation and with the sulfur-containing ligands. The absence of ligand dissociation in the standard simulations (i) and (ii) is also indicative of exaggerated metal–ligand attractions and/or underestimated ligand–ligand repulsions compared with the QM or MK+pol results.

The gas-phase minimized structures were immersed in water and energy-minimized with the MK and Mulliken charges. All L^- ligands remained bidentate, while all protonated LH ligands remained monodentate. The M–O and M–S distances were similar to those obtained in the gas phase (Table 3). However, during a free MD simulation, some of them dissociated or became monodentate. Thus, in order to retain the original coordination of the four ligands, MD in water (vide infra) was carried out, unless otherwise specified, constraining the seven cation–ligand bond distances to their average MM minimized ones.

2.1. MD simulations with Merz–Kollman charges and +3 cation: During the dynamics simulations in water, all com-

plexes coordinated additional water molecules. Selected snapshots are shown in Figure 3. It is seen that the water molecules coordinating to the cations stay close together and two microphases of water and partially hydrophobic ligands are formed around the cation, thereby building an asymmetric environment around it. Without rearrangement of the ligands, no water coordination takes place, as is revealed by the MD simulations with a frozen solute (BELLY option in AMBER).

No internal hydrogen bonds between the ligand proton and the remaining ligand binding sites are formed, in contrast to the gas-phase QM results. Instead of this, second-shell water molecules form hydrogen bonds to these sites (also visible in the snapshots).^[44] As we see from the RDF results (Table 3 and Figure 4), the steric crowding found in the QM calculations is not strong enough to completely hinder water coordination in the molecules studied, including $[YbTP_3TPH]$, for which the QM binding energies already indicated oversaturation. The reason for this may be the compact size and high polarity of the water molecule, as well as the inadequacy of pairwise additive 1-6-12 potentials used. However, some of the results still support the thesis of the

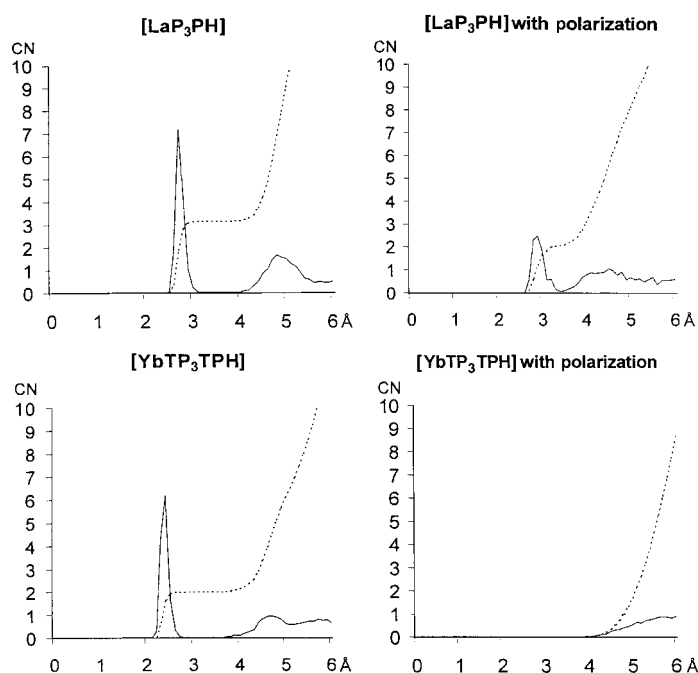


Figure 4. M–O_{water} RDFs (unbroken line) and its integral, the coordination number CN (dotted line; the ordinate gives the CN) of the [ML₃LH] complexes. Simulations in water with the MK charges (left) and MK+pol model (right). Top: La complexes; bottom: Yb complexes.

importance of steric strain for the lanthanide cation coordination. With the dithiophosphinate ligand, the number of coordinated water molecules gradually falls from [LaTP₃TPH] to [YbTP₃TPH]. With the phosphate ligand, on the other hand, the water coordination number in [LaP₃PH] and [EuP₃PH] is about the same, but it gets smaller in [YbP₃PH]. This supports our analysis of the QM energies, which show that steric strain with the dithiophosphinate ligand starts to become important in the Eu³⁺ complex, while for the phosphate ligand only the complex with the small Yb³⁺ cation shows this effect. Yet it is still surprising that both Yb³⁺ complexes coordinate two water molecules, while the QM energies indicated much more steric strain in [YbTP₃TPH] than in [YbP₃PH].

2.2 MD simulations with Mulliken charges as mimics of charge transfer and polarization effects: The reported discrepancies led us to test another set of atomic charges. It would indeed be desirable to use atomic charges that take into account charge transfer and polarization effects, as accounted

for by the QM calculations on the [ML₃LH] complexes. As explained, this can be partially achieved by the use of charges derived independently for each complex. As charges fitted from electrostatic potentials using different fitting procedures may lead to chemically meaningless results,^[45] we decided to use the Mulliken charges as in ref. [15, 46]. As seen in Table S1, the metal charge ranges from 1.51 to 1.76e in the [MP₃PH] complexes, and from 1.28 to 1.34e in the [MTP₃TPH] complexes, the charge transfer from the ligands being generally most pronounced with the hardest cation, Yb³⁺. The polarizations of the coordinated O^{δ-}–P^{δ+} and S^{δ-}–P^{δ+} bonds also differ markedly (about O^{-0.9}–P^{+1.8} and S^{-0.5}–P^{+0.5}), and vary with the metal.

The results for the RDF of water oxygen atoms around the lanthanide cations can be found in Table 3 and Figure 4. The most important outcome is that the problem of water addition to the complexes, which are sterically saturated according to the QM calculations, is still unresolved. While the water coordination numbers CN_w, ranging from 2.5 to 1.0, are somewhat smaller with the Mulliken charges, there still is at least one water molecule coordinated to all complexes, including [YbTP₃TPH], which is already oversaturated in the QM calculations. Furthermore, as with the MK charges, no difference is found for the water coordination of [YbTP₃TPH] and [YbP₃PH]. Therefore, one has to conclude that this approximate representation of electron reorganization effects in the MD simulations does not lead to a better agreement with the QM results.

2.3 MD simulations with MK charges and an explicit polarization energy contribution: The other effect not yet considered that may influence the coordination numbers of the lanthanide cations is the ligand polarization. The high cationic charge is expected to markedly polarize the coordinated ligands. This increases the ligand–ligand repulsions, thereby lowering the coordination numbers compared with unpolarized models.^[42] Therefore, polarization of the solute ligand atoms has been included in some MD simulations. With the MK+pol model, the tendency of the ligands to become monodentate or to totally to dissociate is found to be smaller than in the simulations without polarization. Such a trend has been observed with perchlorate or triflate counterions in solution.^[42] Because of this, we have listed the results of both unconstrained and constrained calculations in Table 4. The most important outcome is that no water coordination occurs in the [YbP₃PH] and [YbTP₃TPH] complexes (Figure 4). On the other hand, water does add to the lanthanum complexes;

Table 4. Complexes simulated by MD in water (MK+pol model). Unconstrained M–X distances in Å (M = La, Eu, Yb; X = O, S binding sites). Number of coordinated water molecules (CN_w) from the unconstrained simulations (CN_{w,UC}) and from the simulations with distance constraints (CN_{w,C}).

Complex ^[a]	M–X1	M–X1'	M–X2	M–X2'	M–X3	M–X3'	M–X4	M–X4'	CN _{w,UC}	CN _{w,C}
[LaP ₃]	2.66	2.54	2.49	3.71	2.47	4.23			5.1	3.8
[LaP ₃ PH]	2.54	2.54	2.49	4.69	2.44	4.46	2.54	4.76	4.5	2.0
[YbP ₃ PH]	2.13	2.13	2.12	2.14	2.13	2.14	2.16	4.11	0.1	
[LaTP ₃]	2.85	2.84	2.82	2.84	2.84	2.85			3.0	3.0
[YbTP ₃]	2.36	2.36	2.36	2.36	2.36	2.36			0.0	
[YbTP ₃ TPH]	2.36	2.35	2.36	2.36	2.36	2.36	10.48	12.34	0.0	0.0

[a] See Table 1.

this confirms the trend of increasing steric strain in the first shell from lanthanum to ytterbium found in the QM calculations. The resulting coordination number is 9 (MK+pol model), instead of 10 with MK charges. As is the case for simulations without polarization, the water addition to lanthanum does lead to the formation of an asymmetric environment around the metal (Figure 5).

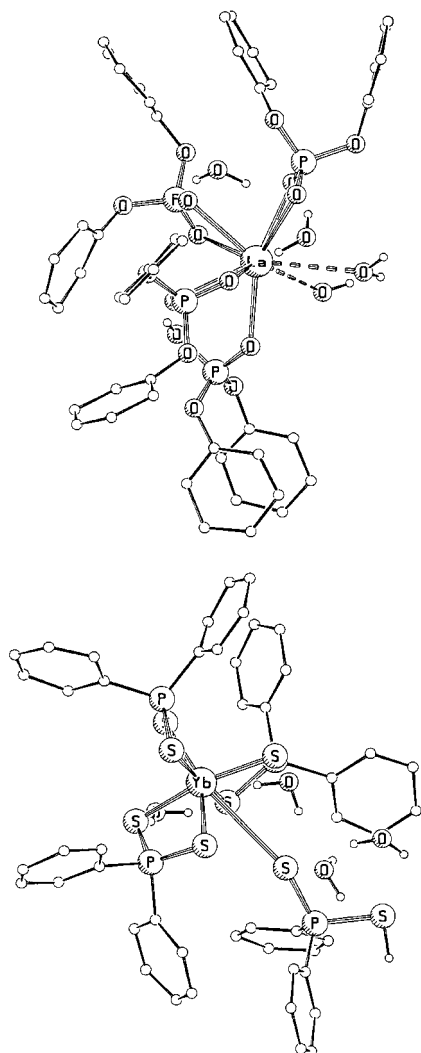


Figure 5. $[\text{LaP}_3\text{PH}]$ (top) and $[\text{YbTP}_3\text{TPH}]$ (bottom) complexes simulated in water using the MK+pol model and constrained M–S or M–O binding distances.

In the QM calculations, the impact of the different binding-site sizes of the PH and TPH ligands is clearly visible. The MD calculations in water with included polarization show the importance of this difference as well. The best example for this is again the difference between the $[\text{YbP}_3\text{PH}]$ and $[\text{YbTP}_3\text{TPH}]$ complexes. In the free MD simulations of these complexes the neutral ligand does dissociate in the case of $[\text{YbTP}_3\text{TPH}]$, where the QM calculation showed that this dissociation is exothermic. On the other hand, in the case of $[\text{YbP}_3\text{PH}]$, the neutral ligand remains bonded to the metal, also in agreement with the QM result. This confirms the importance of the first-shell steric strain caused by the larger

sulfur binding sites of the TP^- and TPH ligands compared with oxygen in P^- and PH for the coordination numbers of the lanthanides.

Conclusion

Two bidentate ligands, one, phosphate, with oxygen atoms as binding sites, the other, dithiophosphinate, with sulfur atoms as binding sites, were compared regarding their ability to form complexes with lanthanide(III) cations, their selectivity for the different cations, and the influence they have on the coordination number in these complexes. In order to study complementary aspects of this problem, we chose to use two different approaches, quantum-mechanical (QM) calculations for model compounds in the gas phase, and simulations with known ligands in the gas phase and in water using molecular dynamics (MD) based on a force-field (FF) energy potential.

As expected from previous studies by our group^[18–20] the QM calculations show that the hard phosphate ligand generally forms stronger complexes than the softer dithiophosphinate ligand, independent of the hardness of the lanthanide cation. Furthermore, as long as there is still enough space left around the cation, both ligands prefer the smaller harder cations over the larger ones, that is, the order of selectivity is $\text{La}^{3+} < \text{Eu}^{3+} < \text{Yb}^{3+}$. This means that in $[\text{ML}_3]$ complexes hard–soft effects do not seem to be of great importance for the lanthanide ion selectivity of the two ligands studied. Nevertheless, additional neutral ligands, which coordinate to the cation, display different affinities: $\text{La}^{3+} < \text{Yb}^{3+} < \text{Eu}^{3+}$ for the phosphate complexes and $\text{Yb}^{3+} < \text{Eu}^{3+} < \text{La}^{3+}$ for the dithiophosphinate complexes. The QM results indicate that this is a consequence of steric strain in the first coordination shell of the cations, a very basic concept which is still almost always neglected in the process of choosing ligands for lanthanide(III) or actinide(III) cations. An analysis of the QM energies suggests that the effect of this steric strain could be as high as 40 kcal mol^{-1} .

It is conceivable that one could use the steric strain in the first shell to avoid unwanted water coordination in solution. In order to test this we carried out MD simulations of the 1:4 complexes in water. However, while the influence of the different binding sites and cation sizes is perceivable in the standard MD calculations as well, it seems to be smaller than in the QM calculations. In particular, in no case was complete hindrance of water coordination achieved. It appears that the steric strain in the first shell cannot be reproduced in MD simulations without the inclusion of polarization effects. An approximate inclusion of electronic rearrangements by means of QM Mulliken charges derived for the full complex only leads to a marginal improvement of the MD vs QM agreement. However, if polarization is included in the MD simulations, the agreement is significantly improved and $[\text{YbP}_3\text{PH}]$ and $[\text{YbTP}_3\text{TPH}]$ do indeed show no more water coordination (whether or not the ligands are constrained), which makes them good candidates for extraction to an organic phase. In the simulations with polarization the impact of steric strain is also visible in the different coordination numbers found for the oxygen- and the sulfur-based ligands, a

result that confirms the different behavior of the binding energies for these two ligand types found in the QM calculations of the complexes with neutral ligands.

Generally, steric effects are thought of as resulting from the size of the atoms or groups of atoms. It is noteworthy that in the MD simulations (*i*) to (*iii*), the size of a given ion and of a given ligand, as determined by the R^* and ϵ van der Waals parameters, remains constant. The contrasting results obtained with the different electrostatic models point to the electrostatic origin of the steric strain in the first coordination shell containing negatively charged ligands or atoms. Of course, in the QM approach, electrostatic and steric effects cannot be separated, as the electron cloud is generally larger for anionic binding sites than for neutral analogues, and larger for sulfur than for oxygen atoms.

Further studies will show whether the effect of blocking water from coordination sites at the metal can be enhanced by combining the first-shell steric strain discussed here with stronger second-shell hydrophobicity, for example by adding additional TBP ligands or large hydrophobic anions, such as are often successfully used in lanthanide/actinide extraction. A related important facet is the alteration of ion extraction efficiency and selectivity by synergistic neutral ligands (e.g. replacing LH by TBP or related derivatives).

From a methodological point of view, our comparison of coordination numbers in vacuo and in an aqueous environment shows that pairwise additive potentials may overestimate the water coordination to complexes with highly charged cations and that addition of polarization energy terms leads to more satisfactory hydration numbers.^[47] This is of particular relevance in the modeling of MRI contrast reagents^[24] and of luminescent complexes.^[25] We also notice that steric strain may be modeled by force-field methods based on a covalent representation of M–L bonds, in conjunction with non-bonded repulsions between the ligand binding sites.^[48–52]

Acknowledgements

The authors are grateful to the EU (Grant Marie Curie F14W-CT98-5003 and F1KWCT2000-0088) and COST D9 for support, and to IDRIS and the Université Louis Pasteur for the allocation of computer resources.

- [1] L. Cecille, M. Casarci, L. Pietrelli, *New Separation Chemistry Techniques for Radioactive Waste and other Specific Applications* (Ed.: Commission of the European Communities), Elsevier Applied Science, London, New York, **1991**.
- [2] A. M. Rozen, B. V. Krupnov, *Russ. Chem. Rev.* **1996**, *65*, 973–1000 and references therein.
- [3] G. R. Choppin, K. L. Nash, *Radiochim. Acta* **1995**, *70/71*, 225–236.
- [4] Y. Zhu, *Radiochim. Acta* **1995**, *68*, 95–98.
- [5] C. Hill, C. Madic, P. Baron, M. Ozawa, Y. Tanaka, *J. Alloys Compd.* **1998**, *271–273*, 159–162.
- [6] G. Modolo, R. Odoj, *Proc. 5th Int. Information Exchange Meeting Actinide Fission Product Partitioning Transmutation* **1998**, 141–151; G. Modolo, R. Odoj, *Solv. Extract. Ion Exch.* **1999**, *17*, 33–53.
- [7] P. S. Mansingh, V. Chakravorty, K. C. Dash, *Radiochim. Acta*, **1996**, *73*, 139–143; J. Chen, Y. Zhu, R. Jiao, *Sep. Sci. Technol.* **1996**, *31*, 2724–2731; Y. Zhu, *Radiochim. Acta* **1995**, *68*, 95–98; G. Jarvinen, R. Barrans, N. C. Schroeder, K. Wade, M. Jones, B. Smith, J. Mills, G. Howard, H. Freiser, S. Muralidharan in *Separations of f Elements* (Eds.: K. L. Nash, G. R. Choppin), Plenum, New York, **1995**, pp. 43–62; C. Hill, C. Madic, P. Baron, M. Ozawa, Y. Tanaka, *J. Alloys Compd.* **1998**, *271–273*, 159–162.
- [8] F. Arnaud-Neu, V. Böhmer, J.-F. Dozol, C. Grüttner, R. A. Jakobi, D. Kraft, O. Mauprivez, H. Rouquette, M.-J. Schwing-Weil, N. Simon, W. Vogt, *J. Chem. Soc. Perkin Trans. 2* **1996**, 1175–1182.
- [9] S. Barbosa, A. G. Carrera, S. E. Matthews, F. Arnaud-Neu, V. Böhmer, J.-F. Dozol, H. Rouquette, M.-J. Schwing-Weill, *J. Chem. Soc. Perkin Trans. 2* **1999**, 719–723.
- [10] L. H. Delmau, N. Simon, M.-J. Schwing-Weill, F. Arnaud-Neu, J.-F. Dozol, S. Eymard, B. Tournois, V. Böhmer, C. Grüttner, C. Musigmann, A. Tunayar, *Chem. Commun.* **1998**, 1627–1628.
- [11] *Hard and Soft Acids and Bases* (Ed.: R. G. Pearson), Dowdon, Hutchinson & Ross, Stroudsburg, PA, **1973**.
- [12] R. D. Hancock, A. E. Martell, *Chem. Rev.* **1989**, *89*, 1875–1914 and references therein.
- [13] R. D. Hancock, A. E. Martell, *Adv. Inorg. Chem.* **1995**, *42*, 89–146.
- [14] L. Troxler, A. Dedieu, F. Hutschka, G. Wipff, *J. Mol. Struct. (THEOCHEM)* **1998**, *431*, 151–163.
- [15] F. Hutschka, L. Troxler, A. Dedieu, G. Wipff, *J. Phys. Chem. A* **1998**, *102*, 3773–3781.
- [16] F. Berny, N. Muzet, L. Troxler, A. Dedieu, G. Wipff, *Inorg. Chem.* **1999**, *38*, 1244–1252.
- [17] M. Baaden, F. Berny, C. Boehme, N. Muzet, R. Schurhammer, G. Wipff, *J. Alloys Compd.* **2000**, *303–304*, 104–111.
- [18] R. Schurhammer, V. Erhart, L. Troxler, G. Wipff, *J. Chem. Soc. Perkin Trans.* **1999**, 2515–2534.
- [19] C. Boehme, G. Wipff, *J. Phys. Chem. A* **1999**, *103*, 6023–6029.
- [20] C. Boehme, G. Wipff, *Inorg. Chem.* **1999**, *38*, 5734–5741.
- [21] J.-C. G. Bünzli, A. Milicic-Tang, *Handbook on the Physics and Chemistry of Rare Earths* (Eds.: K. A. Gschneider Jr., L. Eyring), Elsevier, Amsterdam, **1995**, pp. 306–359 and references therein.
- [22] J.-C. G. Bünzli, B. Klein, G. Chapuis, K. J. Schenk, *J. Inorg. Nucl. Chem.* **1980**, *42*, 1307–1311.
- [23] N. Muzet, E. Engler, G. Wipff, *J. Phys. Chem. B* **1998**, *102*, 10772–10788; M. Baaden, F. Berny, N. Muzet, L. Troxler, G. Wipff, in *Calixarenes for Separation*, ACS Symp. Ser. **2000**, *757* (Eds.: G. Lumetta, R. Rogers, A. Gopalan), ACS, Washington DC, pp. 71–85.
- [24] V. Comblin, D. Gilsoul, M. Hermann, V. Humblet, V. Jacques, M. Mesbahi, C. Sauvage, J.-F. Desreux, *Coord. Chem. Rev.* **1999**, *185–186*, 451–470.
- [25] D. Parker, J. A. G. Williams, *J. Chem. Soc. Dalton Trans.* **1996**, 3613–3628.
- [26] J.-C. G. Bünzli, N. André, M. Elhabiri, G. Muller, C. Piguët, *J. Alloys Compd.* **2000**, *303–304*, 66–74.
- [27] E. Szilagyí, E. Toth, E. Brücher, A. E. Merbach, *J. Chem. Soc. Dalton Trans.* **1999**, 2481–2486.
- [28] M. J. Frisch, G. W. Trucks, H. B. Schlegel, G. E. Scuseria, M. A. Robb, J. R. Cheeseman, V. G. Zakrzewski, J. A. Montgomery Jr., R. E. Stratmann, J. C. Burant, S. Dapprich, J. M. Millam, A. D. Daniels, K. N. Kudin, M. C. Strain, O. Farkas, J. Tomasi, V. Barone, M. Cossi, R. Cammi, B. Mennucci, C. Pomelli, C. Adamo, S. Clifford, J. Ochterski, G. A. Petersson, P. Y. Ayala, Q. Cui, K. Morokuma, D. K. Malick, A. D. Rabuck, K. Raghavachari, J. B. Foresman, J. Cioslowski, J. V. Ortiz, B. B. Stefanov, G. Liu, A. Liashenko, P. Piskorz, I. Komaromi, R. Gomperts, R. L. Martin, D. J. Fox, T. Keith, M. A. Al-Laham, C. Y. Peng, A. Nanayakkara, C. Gonzalez, M. Challacombe, P. M. W. Gill, B. Johnson, W. Chen, M. W. Wong, J. L. Andres, C. Gonzalez, M. Head-Gordon, E. S. Replogle, J. A. Pople, *Gaussian 98, Revision A.5*, Gaussian, Pittsburgh, PA, **1998**.
- [29] T. H. Dunning, P. J. Hay, *Methods of Electronic Structure Theory. Modern Theoretical Chemistry 3* (Ed.: H. F. Schaefer, III), Plenum, New York, **1977**, pp. 1–28.
- [30] M. Dolg, H. Stoll, A. Savin, H. Preuss, *Theoret. Chim. Acta* **1989**, *75*, 173.
- [31] M. Dolg, H. Stoll, A. Savin, H. Preuss, *Theoret. Chim. Acta* **1993**, *85*, 441.
- [32] A. W. Ehlers, M. Böhme, S. Dapprich, A. Gobbi, A. Höllwarth, V. Jonas, K. F. Köhler, R. Stegmann, A. Veldkamp, G. Frenking, *Chem. Phys. Lett.* **1993**, *208*, 111.
- [33] D. A. Pearlman, D. A. Case, J. C. Caldwell, G. L. Seibel, U. C. Singh, P. Weiner, P. A. Kollman, AMBER 4, University of California, San Francisco, **1991**.

- [34] W. D. Cornell, P. Cieplak, C. I. Bayly, I. R. Gould, K. M. Merz, D. M. Ferguson, D. C. Spellmeyer, T. Fox, J. W. Caldwell, P. A. Kollman, *J. Am. Chem. Soc.* **1995**, *117*, 5179–5197.
- [35] F. C. J. M. van Veggel, D. Reinhoudt, *Chem. Eur. J.* **1999**, *5*, 90–95.
- [36] W. L. Jorgensen, J. Chandrasekhar, J. D. Madura, *J. Chem. Phys.* **1983**, *79*, 926–936.
- [37] J. Caldwell, L. X. Dang, P. A. Kollman, *J. Am. Chem. Soc.* **1990**, *112*, 9144–9147.
- [38] J. Applequist, J. R. Carl, K.-K. Fung, *J. Am. Chem. Soc.* **1972**, *94*, 2952–2960.
- [39] E. Engler, G. Wipff, unpublished results.
- [40] E. Engler, G. Wipff, *Crystallography of Supramolecular Compounds* (Ed.: G. Tsoucaris), Kluwer, Dordrecht, **1996**, pp. 471–476.
- [41] J.-M. Lehn, G. Wipff, J. Demuynck, *Chem. Phys. Lett.* **1980**, *76*, 344.
- [42] M. Baaden, F. Berny, C. Madic, G. Wipff, *J. Phys. Chem.* **2000**, *104*, 7659–7671.
- [43] Note that while the differences between the QM and MD structures are somewhat irregular, it can generally be said that they become larger with smaller cations and larger binding sites, i.e. from [LaP₃PH] to [YbTP₃TPH]. This means the difference increases with the steric strain found in the QM calculations.
- [44] These water–ligand hydrogen bonds are much longer in the case of the sulfur ligands. In the M–O_w RDF, these water molecules contribute to the second solvation shell, which shows up as a relatively broad second peak at a distance of about 5 Å. The other water molecules of this shell are hydrogen-bonded to the first-shell water molecules. According to an energy component analysis, the second-shell water molecules hydrogen-bonded to the phosphorus-containing ligands are, owing to their orientation, slightly repulsive towards the metal, and therefore decrease the overall solvation energy of the complex.
- [45] F. Hutschka, Thesis, Université Louis Pasteur, Strasbourg, **1998**.
- [46] J. S. Craw, M. A. Vincent, I. H. Hillier, A. L. Wallwork, *J. Phys. Chem.* **1995**, *99*, 10181–10185.
- [47] T. Kowall, F. Foglia, L. Helm, A. E. Merbach, *J. Am. Chem. Soc.* **1995**, *117*, 3790–3799.
- [48] P. V. Bernhardt, P. Comba, *Inorg. Chem.* **1992**, *31*, 2638–2644.
- [49] P. Comba, *Coord. Chem. Rev.* **1999**, *185–186*, 81–98.
- [50] P. Comba, *Coord. Chem. Rev.* **1999**, *182*, 343–371.
- [51] B. P. Hay, *Coord. Chem. Rev.* **1993**, *126*, 177–236 and references therein.
- [52] J. Beech, M. G. B. Drew, P. B. Leeson, *Struct. Chem.* **1996**, *7*, 153–165.

Received: September 8, 2000 [F2721]